IEEE Access
Multidisciplinary : Rapid Review : Open Access Journal

Received 8 July 2024, accepted 15 July 2024, date of publication 18 July 2024, date of current version 26 July 2024.

Digital Object Identifier 10.1109/ACCESS.2024.3430862

RESEARCH ARTICLE

Comparative Analysis of Metaheuristics for Solving the Optimal Power Flow With Renewable Sources and Valve-Point Constraints

GERARDO CASTAÑÓN[1], (Senior Member, IEEE), ANA MARIA SARMIENTO[1], (Member, IEEE), ALBERTO F. MARTÍNEZ-HERRERA[1], (Member, IEEE), ALEJANDRO ARAGÓN-ZAVALA[2], (Senior Member, IEEE), FERNANDO LEZAMA[3], (Senior Member, IEEE), AND ZITA VALE[3], (Senior Member, IEEE)

[1]School of Engineering and Sciences, Tecnológico de Monterrey, Monterrey, Nuevo Leon 64849, Mexico
[2]Department of Electronics and Mechatronics, Tecnológico de Monterrey, Queretaro Campus, Santiago de Querétaro, Queretaro 76130, Mexico
[3]GECAD—Research Group on Intelligent Engineering and Computing for Advanced Innovation and Development, LASI—Intelligent Systems Associate Laboratory, Polytechnic of Porto, 4200-072 Porto, Portugal

Corresponding author: Fernando Lezama (flz@isep.ipp.pt)

This work was supported by GECAD Research Center under Grant UIDB/00760/2020, DOI: 10.54499/UIDB/00760/2020.

ABSTRACT The Optimal Power Flow (OPF) problem, used to obtain efficient operation conditions with the lowest cost or the minimum power loss in electrical power systems, is a non-polynomial problem that becomes even harder to analyze when considering renewable energy sources (RES) with uncertain behavior. Therefore, establishing a manageable number of RES scenarios in the modeling is essential for optimizing cost-effective solutions, including those with constraints such as the valve-point effect and prohibited operational zones. This work compares three differential evolution algorithm (DEA) variants and four well-known metaheuristics: the Particle Swarm Optimization (PSO), the Bio-geographical Based Optimization (BBO), the Artificial Bee Colony Optimization (ABC), and the Non-dominated Sorting Genetic Algorithm II (NSGA-II). The metaheuristics are compared: 1) to determine the one with the best performance considering RES; 2) to establish an approach to minimize and find the best set of scenarios representing variable RES; 3) to compare the success rate of convergence of the penalized function against the real objective function. Results show that BBO and PSO optimization are the best choices for solving the classic objective function of OPF. On the other hand, the DE/best/1 (DEAB) algorithm demonstrates the best performance when the valve-point effect with prohibited zones is considered. DEAB presents the largest weighted cumulative rating (WCR) and the second-best weighted cumulative successful rate (WCSR) for all the evaluated criteria.

INDEX TERMS Differential evolution algorithm, electrical power systems, optimal power flow, renewable energy sources, stochastic modelling.

I. INTRODUCTION

Renewable energy sources (RESs) have emerged as a viable alternative to fossil fuels, driven by concerns over climate change and the depletion of fossil energy sources [1]. However, deploying RESs introduces new challenges and constraints, necessitating reevaluating the modeling process due to its stochastic nature and the limited availability of certain sources [2]. For example, while hydroelectric power has contributed to global electricity generation, dry dam

The associate editor coordinating the review of this manuscript and approving it for publication was Fabio Mottola.

scenarios in various countries threaten its reliability. These extreme conditions highlight the importance of planning for scenarios where RESs are temporarily unavailable to ensure an uninterrupted power supply [3], [4].

The optimal power flow (OPF) plays a crucial role in electrical engineering, serving various functions across the operation and planning of power systems [5]. Solving the OPF ensures the efficient and reliable management of electrical networks by optimizing power generation, transmission, and distribution assets while balancing economic efficiency, system reliability, and environmental sustainability. Integrating RESs into OPF poses unique challenges due to their stochastic and time-varying behavior. Factors such as the availability of sunlight and wind speed introduce variability that must be accounted for in network planning [6]. While much of the existing literature focuses on minimizing monetary costs, power losses, pollutant emissions, and voltage instability, the incorporation of RESs fundamentally alters the optimization objectives of OPF [7].

Thus, the OPF problem formulation must be extended to incorporate RES. Various methodologies, including mixed-integer nonlinear programming [8], evolutionary algorithms, and swarm intelligence [9], are employed to tackle OPF challenges. These approaches are validated through simulations, often using probabilistic models to represent stochastic elements such as wind and solar generation. These OPF methodologies are critical to the state-of-the-art (briefly analyzed in Sect. II), providing insights into optimizing power system operation in the face of evolving energy landscapes.

Within that context, the contributions of this work are the following: to determine which of the tested metaheuristic algorithms has the best performance for each case, with the addition of RESs and the success rate of convergence of the penalized function against the real objective function. We test three variants of the differential evolution algorithm (DEA) [10] along with four well-known metaheuristics: the Particle Swarm Optimization (PSO) [11], the Bio-geographical Based Optimization (BBO) [12], the Artificial Bee Colony Optimization (ABC) [13], and the Non-dominated Sorting Genetic Algorithm II (NSGA-II) [14]. Using the methodology and the algorithms benchmark presented by Castañón et al. [10], we rank the tested metaheuristics (low-high sorting ranking) along with the computation of a success rate ranking to determine the best-performing algorithm. We present a classical OPF statement to evaluate the impact on each metaheuristic when including RES before adding tight constraints involving the valve-point loading effect and prohibited operating zones. Typical statistics like mean, minimum, and maximum values are the baseline for rating each metaheuristic. Additionally, the success rate of convergence is obtained for each metaheuristic and each scenario that the RESs generate.

This work is organized as follows: Section II revise state-of-the-art applications of metaheuristic algorithms solving the OPF. Section III details the description of the OPF, the constraints, and the objective functions to be solved by including penalization factors, valve-point effects, prohibited zones, and the use of RESs. Section IV describes the DEA used in this work. Section V describes the IEEE-30 electric network tested as the main scenario and the methodology used to apply the DEA versions. Section VI describes the results obtained with the DEA versions to determine the ranking and presents the respective discussions of those results. Finally, Section VII presents the conclusions of this work.

II. STATE OF THE ART

The OPF problem aims to achieve efficient operations with minimized costs or losses. With the increasing integration of RESs, the challenge lies in accurately modeling their stochastic behavior and proposing effective tools to solve the resulting complex problem. This section provides a chronological review of recent advancements in OPF optimization, highlighting the evolution of methodologies and approaches over time.

In [15], Hu et al. expanded the energy generation capacity of the IEEE 24-bus network using a combination of gas, thermal, and wind energy sources, with wind being the stochastic component. Windmill farms and most RES sources are modeled using the Weibull probability density function (PDF). Additional electric lines are incorporated to enhance network performance. The multi-objective NSGA-II algorithm is applied to minimize investment, production, and carbon emission costs.

In [16], Mohseni-Bonab et al. addressed the stochastic multi-objective optimal reactive power dispatch (SMO-ORPD) problem. They modeled the IEEE-57 network deterministically to solve voltage stability and power losses, computing their Pareto fronts. Then, load scenarios were derived from a normal PDF, while wind power scenarios used a Raleigh PDF [17]. Instead of two regions (shortage or surplus), the PDFs were divided into five regions with respective probabilities.

In [18], Khaled et al. used a modified Particle Swarm Optimization (PSO) algorithm to design a deterministic 24-hour model for the OPF problem, including RES. The PSO was compared to Tabu Search and a Genetic Algorithm. Each RES was modeled as an hourly variable power source. The IEEE-30 network was analyzed, replacing thermal sources with PV farms. Additionally, wind turbines were placed on buses 7 and 12. The authors found that RES significantly reduced costs, power loss, and total power generation.

Reddy and Bijwe [19] present a similar approach by solving the OPF as the Real-Time OPF (RT-OPF) and the Day-Ahead OPF (DA-OPF) with shorter time intervals of 1-10-15 minutes, during an hour, for a complete day. The main goal is to maximize the profit inside the electric network. The IEEE-30 electric network is considered as the case study. MATLAB Optimization Toolbox (FMINCON function) was used to obtain the results.

Maulik and Das [20] studied the OPF problem in an AC-DC hybrid microgrid with RES. The first AC section includes a natural gas turbine, biomass cell, and wind turbine, while the second section includes a natural gas fuel cell, solar farm, and biomass. They formulated a multi-objective problem considering cost and emissions, solved using PSO and the fuzzy max-min technique. The wind farm is modeled with a Weibull PDF, the solar farm with a beta PDF, and the load with a normal PDF.

Elattar et al. [21], [22] extended the OPF problem by including heat units and wind energy sources. They modeled wind energy based on [23], considering underestimation (surplus), overestimation (shortage), and direct cost scenarios. A modified Moth Swarm Algorithm (MMSA) was proposed to minimize operating costs and transmission power loss and improve voltage profiles for IEEE-30 and IEEE-118 networks in [21]. Later, a modified JAYA algorithm was used to solve the multi-objective OPF, minimizing fuel cost, emission cost, and power losses [22].

Awad et al. [24] developed a modified DEA to solve the Optimal Active-Reactive Power Dispatch (OARPD). The new DEa-AR algorithm shows fast convergence compared to other metaheuristics like CEEPSO and ICDE. The authors included RESs such as wind farms (Weibull PDF), solar farms (log-normal PDF), and hydro generators (Gumbel PDF), but only the wind farm modeling is explicitly included in the objective function, considering underestimation, overestimation, and direct cost scenarios, similar to [21] and [23]. The IEEE-57 network was used for testing, with 6 cases, 31 runs per case, and 50,000 evaluations per run.

Biswas et al. [25] simulated a stochastic ORPD model with wind and solar RESs on the IEEE-30 network. They used Weibull and log-normal PDFs to model the wind and solar farms. Using a Monte Carlo approach, 1000 scenarios (reduced to 25) of load, wind, and solar generation were created, and the problem was solved 25 times using Success History-based Adaptive Differential Evolution with Epsilon Constraint (SHADE-EC) to optimize power losses and voltage deviation. The deterministic ORPD problem without RESs was also solved using SHADE-EC for the IEEE-30 and IEEE-57 networks.

Recent advancements in OPF optimization techniques include Li et al. work [26] using an enhanced adaptive differential evolution (JADE) framework, promising improved performance with self-adaptive penalty constraint handling; Li et al. [27] work on uncertainty management into OPF with stochastic RES; Naderi et al. [28] introducing a hybrid self-adaptive heuristic for versatile single and multi-objective OPF problems; Sarda et al. [29] developing a dynamic OPF framework using cross-entropy covariance matrix adaptation for integrating electric vehicles and renewables; and Kahraman et al. [30] exploring diverse solution spaces with a multi-objective manta ray foraging optimizer for OPF.

Also, recently, hybridization has emerged as an effective approach to tackle the complexity of OPF problems with RES integration. For instance, Nadimi-Shahraki et al. [31] combined whale and moth-flame optimization algorithms for enhanced performance. Mohamed et al. [32] proposed a hybrid gradient-based optimizer with moth-flame optimization, demonstrating synergy between traditional and nature-inspired techniques. Hassan et al. [33], [34] introduced enhanced hunter-prey optimization and wild horse optimizer variants for OPF with RES and FACTS devices. Sarda et al. [35] presented a hybrid cross entropy-cuckoo search algorithm, highlighting the versatility of integrating different nature-inspired approaches for solving OPF problems.

TABLE 1. Summary of the objective functions abbreviations and definitions.

- slack : Slack bus.
- NL : Number of load buses.
- nl : Number of load lines.
- NT : Number of taps.
- NG : Number of generators.
- NTG : Number of thermal generators.
- NB : Number of buses.
- NC : Number of shunts.
- P^{NG} is a vector : Real power injected to the network, where p_{slack} is the power obtained in the node identified as the slack bus.
- V^{NG} is a vector : Voltage magnitude to the network.
- Q^{NC} is a vector : Reactive power injected with a shunt device.
- Q^{NG} is a vector : Reactive power injected to the network.
- T^{NT} is a vector : Tap of the transformer.
- V^{NL} is a vector : Voltage magnitude of the load buses.
- S^{nl} is a vector : Total power that a load line can hold.

Finally, in a comparative analysis by Castañón et al. [10], various nature-inspired algorithms, including the Differential Evolution algorithm (DEA), were evaluated addressing the OPF problem without RES. The study sheds light on the effectiveness of DEA as a benchmark algorithm, emphasizing the importance of algorithmic selection and fine-tuning for optimal results. Furthermore, it suggests future research directions to integrate RES into the OPF formulation to enhance its applicability in modern power systems.

In summary, our work bridges gaps in the current research landscape by evaluating the performance of metaheuristic algorithms in solving OPF problems with RES integration. Building upon established methodologies, we assess the effectiveness of several algorithms, including variants of the DEA and other metaheuristics. By extending the analysis to incorporate tight constraints and considering the success rate of convergence, our work provides valuable insights into algorithmic performance under diverse scenarios.

III. DESCRIPTION OF THE PROBLEM

Let $f(x, u)$ be the objective function, $\mathbf{x}$ a vector of independent variables, and $\mathbf{u}$ the vector of dependent ones. The OPF can be described as [36], [37], and [38]:

Definition 1: Minimize :

$$f(\mathbf{x}, \mathbf{u}) \tag{1}$$

subject to :

$$g(\mathbf{x}, \mathbf{u}) \leq 0 \tag{2}$$
$$h(\mathbf{x}, \mathbf{u}) = 0 \tag{3}$$

where $g(\mathbf{x}, \mathbf{u}) \leq 0$ refers to the inequality constraints and $h(\mathbf{x}, \mathbf{u})$ are equality constraints. These constraints apply to vectors $\mathbf{x}$ and $\mathbf{u}$. The mathematical expression of $\mathbf{x}$ is as follows:

$$\mathbf{x} = [\mathbf{P}^{NG}\mathbf{V}^{NG}\mathbf{Q}^{NC}\mathbf{T}^{NT}] \tag{4}$$

where the first set of components, i.e., $\mathbf{P}^{NG}$ and $\mathbf{V}^{NG}$, is related to the power generation and voltage magnitude, respectively. $\mathbf{P}^{NG}$ is formed by the components p_m and $\mathbf{V}^{NG}$ is formed by the components v_m^{NG}. Then, each component is delimited as:

$$v_m^{min} \leq v_m^{NG} \leq v_m^{max} \tag{5}$$
$$p_n^{min} \leq p_n^{NG} \leq p_n^{max} \tag{6}$$

where $m \in \{1, .., NG\}$ and $n \in \{2, .., NG\}$. The next set of components is related to the shunt constraints stored at $\mathbf{Q}^{NC}$, with each component defined as:

$$q_i^{min} \leq q_i^{C} \leq q_i^{max} \tag{7}$$

where $i \in \{1, .., NC\}$. Finally, the components that belong to the transformers $\mathbf{T}^{NT}$ are denoted as t^{NT}, defined as:

$$t_k^{min} \leq t_k^{NT} \leq t_k^{max} \tag{8}$$

where $k \in \{1, .., NT\}$. In this work, $\mathbf{x}$ will be treated as an individual (i.e., a solution) of a population of solutions for each tested metaheuristic.

On the other hand, the mathematical expression for the vector of dependent variables $\mathbf{u}$ is:

$$\mathbf{u} = [p_{slack}\mathbf{V}^{NL}\mathbf{Q}^{NG}\mathbf{S}^{nl}] \tag{9}$$

where p_{slack} the power obtained in the slack bus p_{slack}, $\mathbf{V}^{NL}$ and $\mathbf{Q}^{NG}$ and $\mathbf{S}^{nl}$ is the maximum load of the network lines. Then, their operation limits are denoted as:

$$p_{slack}^{min} \leq p_{slack} \leq p_{slack}^{max} \tag{10}$$
$$q_m^{min} \leq q_m^{NG} \leq q_m^{max} \tag{11}$$

Finally, the security constraints are also included in $\mathbf{u}$ as:

$$v_o^{min} \leq v_o^{NL} \leq v_o^{max} \tag{12}$$
$$s_l \leq s_l^{max} \tag{13}$$

where $o \in \{1, .., NL\}$, $l \in \{1, .., nl\}$. s_l is the absolute value of the complex number that relates the real and reactive power, i.e., $s_l = |p_l + jq_l|$ and it must be lower than the power allowed on each line of the network. In this manuscript, $\mathbf{u}$ is the vector used to compute the penalization factors in the objective function.

Following the modeling, $h(\mathbf{x}, \mathbf{u})$ refers to the power balance inside the network to be analyzed. These equations are described as follows [36], [37]:

- For $\mathbf{P}^{NG}$

$$p_m^G = p_m^d + v_m \sum_{n=1}^{NB} v_n[g_{m,n}cos(\theta_m - \theta_n) + b_{m,n}sin(\theta_m - \theta_n)] \tag{14}$$

- For $\mathbf{Q}^{NG}$

$$q_m^G + q_m^C = q_m^d + v_m \sum_{n=1}^{NB} v_n[g_{m,n}sin(\theta_m - \theta_n) - b_{m,n}cos(\theta_m - \theta_n)] \tag{15}$$

where p_m^G, q_m^G are the injected powers, p_m^d, q_m^d are the loads and $g_{m,n}$, $b_{m,n}$ are the conductance and susceptance of the load presented between the nodes m, n.

A. RENEWABLE ENERGY SOURCES CHARACTERIZATION AND THEIR INCLUSION IN THE OBJECTIVE FUNCTIONS

Unlike the typical modeling of the OPF, stochastic aspects arise when RESs are included. Following [25], the windmill farm is modeled as a piecewise function:

$$p_w(v_w) = \begin{cases} 0 & \text{for } v_w < v_{w,in} \text{ and } v_w > v_{w,out} \\ p_{wr}\dfrac{(v_w - w_{w,in})}{(v_{w,r} - v_{w,in})} & \text{and } v_{w,in} \leq v_w \leq v_{w,r} \\ p_{wr} & \text{for } v_{w,r} < v_w \leq v_{w,out} \end{cases} \tag{16}$$

where the stochastic components can be obtained from the Weibull PDF as:

$$\Delta_v(v_w) = \left(\frac{\beta}{\alpha}\right)\left(\frac{v_w}{\alpha}\right)^{\beta-1} exp\left[-\left(\frac{v_w}{\alpha}\right)^{\beta}\right] \tag{17}$$

Here, the stochastic component v_w represents the velocity of the wind that generates the power to be delivered to the electric network. Fig. 1(a) shows a Monte Carlo approach to obtain samples when using Eq. 16, and Fig. 1(b) shows how Eq. 17 behaves. Eq. 17 has four segments that are appreciated in Fig. 1(b). Two of them have a zero value before $v_{w,in}$ and after $v_{w,out}$, one of them has a linear behavior between $v_{w,in}$ and $v_{w,r}$, and the remainder region is constant.

The load of the network is established as a random variable and modeled as a normal PDF as follows:

$$\Delta_d(P_d) = \frac{1}{\sigma_d\sqrt{2\pi}} exp\left[-\frac{(p_d - \mu_d)^2}{2\sigma_d^2}\right] \tag{18}$$

where p_d is the stochastic component.

We use eq. 19 to determine the RES cost for the wind case [39]:

$$c(P_w) = d_w(P_w) \tag{19}$$

On the other hand, the power delivered by the PV solar farm is modeled by a piecewise function as:

$$P_s(G_s) = \begin{cases} P_{sr}\left(\dfrac{G_s^2}{G_{std}R_c}\right) & \text{for } 0 < G_s < R_c \\ P_{sr}\left(\dfrac{G_s}{G_{std}}\right) & \text{for } G_s \geq R_c \end{cases} \tag{20}$$

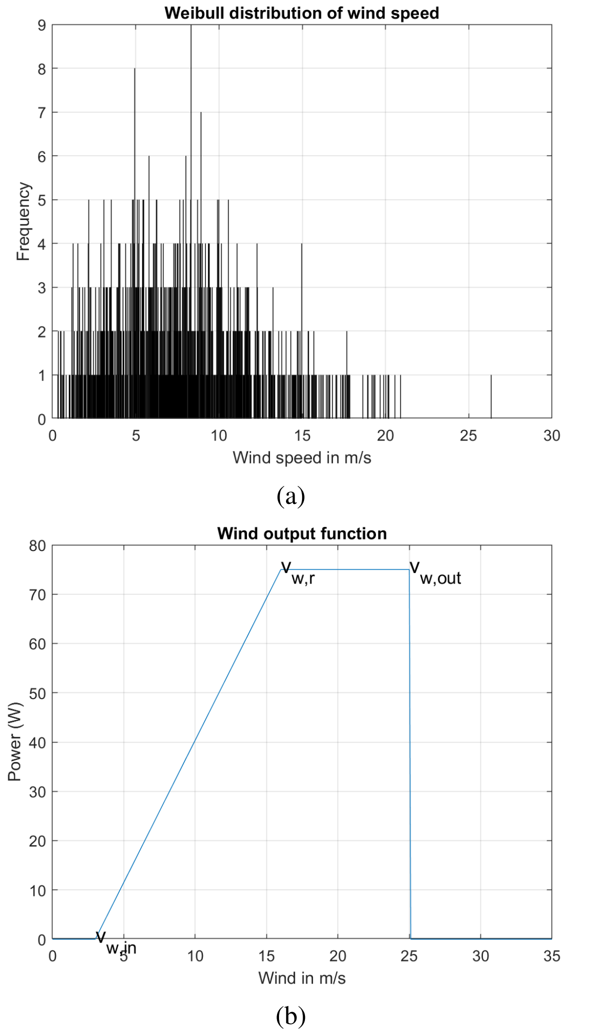

FIGURE 1. **(a) Stochastic behavior and (b) power profile for windmill farm, obtained by following the steps found in [25].**

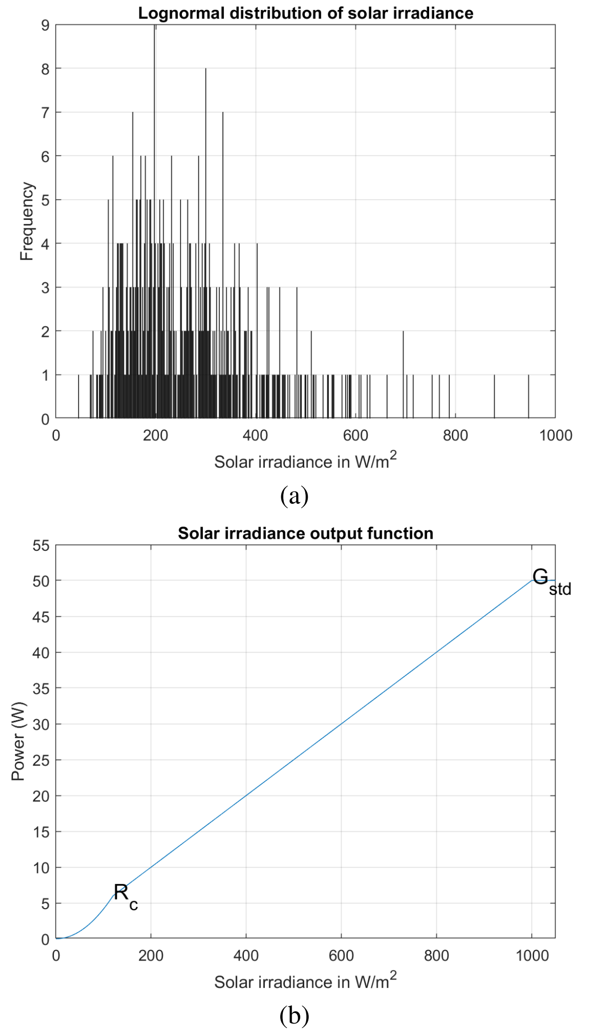

FIGURE 2. **(a) Stochastic behavior and (b) power profile for the solar farm, obtained by following [25].**

where the stochastic behavior is obtained from a lognormal PDF as:

$$\Delta_G(G_s) = \frac{1}{G_s\sigma_s\sqrt{2\pi}} exp\left[-\frac{(ln(G_s)-\mu_s)^2}{2\sigma_s^2}\right] \quad (21)$$

Here, the stochastic component G_s is the irradiance that the solar farm receives to generate the power to be delivered to the electric network. Fig. 2(a) shows a Monte Carlo approach to obtain some samples when using Eq. 21, and Fig. 2(b) shows how Eq. 20 behaves. The first part of Eq. 20 behaves as a quadratic chart, and after the R_c reference behaves as a linear one. The linear behavior is limited by the power of the source that can be produced. If such a limit is surpassed, then the limit of the source is the maximum value.

To determine the cost of the RES for the solar case, we use Eq. 22 [39]:

$$c(P_e) = h_e(P_e) \quad (22)$$

The respective values for $d_w = 1.6$ and $h_e = 1.6$ can be found in [39]. In this way, it is possible to establish two scenarios. The first one is to minimize the cost function, represented as [39]:

$$f_1(x) = \sum_{i=1}^{NTG} a_i + b_i p_i^G + c_i(p_i^G)^2 + \ldots d_w(P_w) + h_e(P_e)(\$/h) \quad (23)$$

where the respective solar and wind sources are included. The same approach can be used when the goal is to minimize the total cost function with valve-point effect and prohibited zones [38], [39]:

$$f_2(x) = \sum_{i=1}^{NTG} a_i + b_i p_i^G + c_i(p_i^G)^2 + \ldots |d_i \times sin\left[e_i \times (p_i^{min} - p_i^G)\right]| + \ldots d_w(P_w) + h_e(P_e)\ (\$/h) \quad (24)$$

Nevertheless, typically $f_1(x)$ and $f_2(x)$ are extended with the use of penalty factors to control the dependent variables efficiently [40]. Then, $f_1(x)$ and $f_2(x)$ become $f_1(x, u)$ and $f_2(x, u)$. For instance, $f_1(x, u)$ is expressed in Eq. 25 as:

$$f_1(x, u) = f_1(x) + \lambda_P(p_G^{slack} - p_{lim}^{slack})^2 + \dots \\ \lambda_V \sum_{o=1}^{NL}(v_o^L - v_o^{lim})^2 + \dots \\ \lambda_Q \sum_{m=1}^{NG}(q_m^G - q_m^{lim})^2 + \dots \\ \lambda_S \sum_{l=1}^{nl}(|s_l| - s_l^{max})^2 \tag{25}$$

where $f_1(x)$ is the function to be evaluated and:

$$u^{lim} = \begin{cases} u^{max}, & u > u^{max}; \\ u^{min}, & u < u^{min}; \\ u, & \text{otherwise.} \end{cases} \tag{26}$$

To obtain $f_2(x, u)$, $f_1(x)$ is substituted with $f_2(x)$. In Eq. 26, if a quantity is below u^{min} or it is larger than u^{max}, then the difference between the quantity and its respective limit is computed. Otherwise, the difference must be zero because the quantity is subtracted by itself. As explained in this section, the elements to be penalized belong to **u**. Additionally, s_l^{max} is the maximum supported power in the branch l, while $|s_l|$ is the maximum absolute power for the same line. Such value is taken from the maximum computed quantity when the flow is computed in both directions of l [38], [40].

IV. DIFFERENTIAL EVOLUTION ALGORITHM

The Differential Evolution algorithm (DEA) is one of the most implemented metaheuristics to solve NP-like problems. Storn and Price introduced DEA in 1997 [41], and since then, different problems have been solved successfully with this method. Typically, five steps are considered to generate candidate solutions that help obtain sub-optimal solutions.

Initially, candidate solutions denoted as individuals are generated randomly. Each individual is a vector evaluated in the objective function to obtain an output. For the problem presented in this manuscript, each individual is $\mathbf{x}_i$ with length $D = 24$. The individuals are then stored in a population matrix, or *Pop*, where the number of individuals is *Np*.

The mutation operation is a weighted equation of differences expressed in Eq. 27 as:

$$m^i = x^{r1} + M(x^{r2} - x^{r3}) \tag{27}$$

where $M \in (0, 1)$ is the mutation constant and m^i is the mutant vector. We conducted a parametric analysis to determine the optimal mutation and recombination constants that minimize power loss, aligning with the recommendations provided in [42] where Islam et al. recommend using $M = 0.8$. Eq. 27 is known as DE/Rand/1 version, where three individuals are chosen randomly. These individuals are denoted as $x^{r1}, x^{r2}, x^{r3} \in \{1, \dots, Np\}$, which are different to the current individual x^i. Eq. 27 is not the only way to determine the mutation operation. For instance, in Eq. 28 the best element (*best*) in the population *Pop* is taken instead of $r1$ as:

$$m^i = x^{best} + M(x^{r1} - x^{r2}) \tag{28}$$

This is also known as DE/Best/1 version.

The recombination step is summarized in Eq. 29 as:

$$t^{i,j} = \begin{cases} m^{i,j} & \text{if } rand \le Cr \text{ or} \\ & Rnd = j \; \forall j \in \{1, \dots, D\} \\ x^{i,j} & \text{otherwise} \end{cases} \tag{29}$$

where $Cr \in (0, 1)$ is the recombination constant and its recommended value, following [42], is set to $Cr = 0.9$. A new candidate vector t^i is formed with the recombination of the mutant vector and the current target vector x^i. Such recombination is based on two random numbers; one of them $(rand)$ is compared to Cr and the other one (Rnd) is compared to the current component of the vectors ($j \in \{1, \dots, D\}$). If $rand \le Cr$ or $Rnd = j$, then the component coming from the mutant vector $m^{i,j}$ is stored in $t^{i,j}$, otherwise $x^{i,j}$ is stored.

Notice that t^i may have components outside the bounds of the variables when mutation and recombination are applied. Thus, if any element of $t^{i,j}$ is outside their respective bounds, a new value between the respective bounds can be generated randomly.

The selection step is described as:

$$Pop_i = \begin{cases} t^i & \text{if } f(t^i, u^i) < f(x^i, u^i) \\ x^i & \text{otherwise ,} \end{cases} \tag{30}$$

In this step, the trial vector t^i is added to *Pop* if the value of the objective function (either $f_1(x, u)$ or $f_2(x, u)$) obtained with it is lower than the obtained with the target vector x^i. Otherwise, x^i remains in *Pop*. In this way, a new *Pop* is obtained at each iteration (also called "generations" in DEA) $g \in \hat{G}$ with $\hat{G}$ as the total number of generations.

A variant tested in this manuscript considers a new strategy to enhance the DEA with the Adaptive Guided Differential Evolution (AGDEA) [43]. The main features in this DEA version are related to the mutation and recombination steps, where Cr is adapted to generate the best recombination strategy, and the population is sorted in such a way that the best individuals guide the worst ones, rather than random selections as it is done for the typical mutation strategies $DE/rand/1$ and $DE/best/1$.

The general pseudo-code for DEA applied to OPF is shown in Algorithm 1. The output of the algorithm includes the best vector candidate in the population when the total generations $\hat{G}$ have been executed Pop_{best}; the function evaluations with the penalty factors *Fitness*; and the function evaluation without these penalty factors *FitnessNoPenalty*. The function evaluations stored in *Fitness* and *FitnessNoPenalty* are related to the best results obtained for each $g \in \hat{G}$.

Algorithm 1 DEA Applied to OPF

procedure DEA
  Input the control parameters for DEA
  Build initial population *Pop*
  Evaluate fitness for each individual in *Pop*
  Begin generations counter $g = 1$
 for $g = 1$ *to* $\hat{G}$ **do**
  for $i = 1$ *to* Np **do**
   Generate random individuals.
   Do mutation m^i according to Eq. 27 (or another variant);
   Recombination to obtain t^i. Eq. 29;
   Validate t^i.
   Update t^i if needed;
   Solve t^i with Newton-Raphson (MATPOWER);
   Apply selection operator Eq. 30;
  end for
 end for
 Pop_{best} obtained with the lowest fitness.
 return Pop_{best}, *Fitness*, *FitnessNoPenalty*
end procedure

V. METHODOLOGY AND THE ANALYZED SCENARIO

The main goal of the methodology is for the DEA to be able to eliminate penalization factors when evaluating a given objective function. That means if $f_1(x, u) - f_1(x) = 0$ or $f_2(x, u) - f_2(x) = 0$, the trial is considered successful, otherwise such trial is considered a "failure" because the penalization factors are still present in the objective function as residuals. To achieve the main goal, the components of $\mathbf{u}$ are subtracted from their respective limits as shown in Eq. 26 when $\mathbf{u}$ is evaluated in $f_1(x, u)$ or $f_2(x, u)$ as expressed in Eq. 25. The components in $\mathbf{u}$ are obtained when solving the system with the Newton-Rapshon method. Then, it is expected that the more function evaluations through generations are done, the more penalization functions will be mitigated until a zero value for all of them is achieved. Because each metaheuristic has a stochastic behavior, sufficient tests are needed to determine the number of successful trials. Then, 100 trials are launched for each scenario where their respective statistics are computed (mean, maximum, and minimum values).

The electric network tested is the IEEE-30 network, formed by one slack bus, five PV buses (injected power), and $NL = 24$ PQ buses (load buses). Then, there are $NB = 30$ buses when adding all of these buses. Additionally, there are $nl = 41$ lines. Compared to the electric network implemented in Abou et al. [36], the schematic presented in Fig 3 includes the RESs as proposed by Biswas et al. [25], where the bus 5 is powered with a windmill farm, and the bus 8 is powered by a solar farm. To do the respective analysis, MATLAB-R2023a was used to configure the IEEE-30 network with MATPOWER 6.0 [44], [45].[1] It is important to mention that several tests were performed using earlier versions of MATLAB, and no significant differences in processing time were observed. The reader interested in a comprehensive statistical analysis of the running times for the solution algorithms is referred to [10]. The parameters for the wind source are: $v_{w,in} = 3m/s$, $v_{w,r} = 16m/s$, $v_{w,out} = 25m/s$ and $p_{wr} = 75$; and for the solar source are: $p_{sr} = 50$, $G_{std} = 1000W/m^2$ and $R_c = 120W/m^2$.

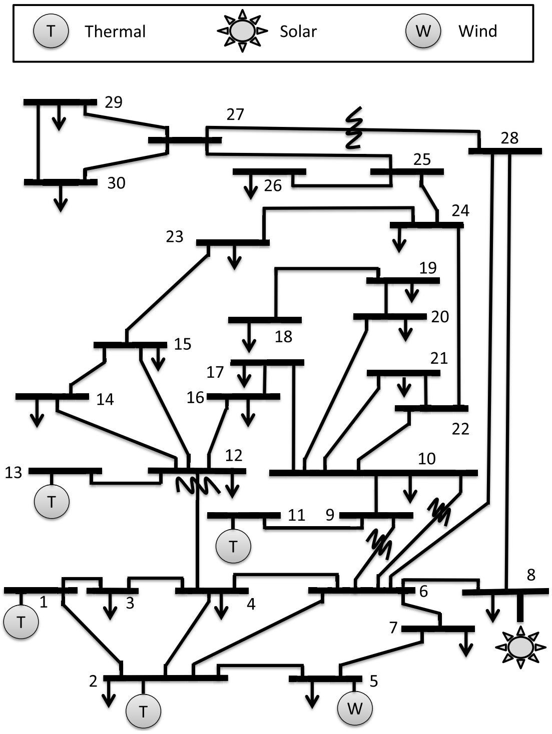

FIGURE 3. IEEE-30 network based on [25] and [36].

Table 2 shows the scenarios generated using Monte Carlo simulation and the backward algorithm [25]. A set of $N_0 = 1000$ coordinates were generated as $[p_d, v_w, G_s]$, to later reduce the value of 1000 coordinates to 25 ones. For p_d, the normal PDF was implemented with ($\mu = 70, \sigma = 10$); for v_w, the Weibull PDF was used with ($\alpha = 9, \beta = 2$). For G_s, 500 elements were generated with the lognormal PDF with ($\mu = 5.5, \sigma = 0.5$) because there is no solar source available half of the day, and therefore, the remaining 500 elements are set to zero. The following commands in MATLAB were used to generate each element of $[p_d, v_w, G_s]$, respectively: $normrnd(muv, sigmav, 1, 1000)$ (being muv and $sigmav$, $\mu = 70$ and $\sigma = 10$, respectively), $wblrnd(alpha, beta, 1, 1000)$ (being $alpha$ and $beta$, $\alpha = 9$ and $\beta = 2$, respectively) and $lognrnd(mu, sigma, 1, 500)$ (being mu and $sigma$, $\mu = 5.5$ and $\sigma = 0.5$, respectively), where for G_s the 500 elements with zero are attached and randomly permuted with those 500 elements generated by *lognrnd*. Columns 5 and 6 of Table 2 show the power outputs obtained from the wind and solar sources, respectively. The last column shows the probability of occurrence of each scenario.

Table 3 shows the parameters that are involved in evaluating the slack bus (position 1) and the PV buses

[1] Available for download in http://www.pserc.cornell.edu/matpower/.

TABLE 2. Own set of scenarios generated with the backward algorithm from [25].

Scenarios	$p_d(\%)$	$v_w(m/s)$	$G_s(W/m^2)$	P_w	P_s	Probability
1	58.6127	2.5858	877.0411	0	43.8521	0.0010
2	64.7924	3.5443	515.6340	3.1403	25.7817	0.0040
3	68.6754	6.5052	196.5254	20.2220	9.8263	0.0600
4	66.1084	4.8020	131.1691	10.3964	6.5585	0.0700
5	61.0908	14.0247	73.9610	63.6043	2.2793	0.0040
6	78.1179	16.4379	607.0791	75.0000	30.3540	0.0020
7	63.3731	9.9471	583.4297	40.0795	29.1715	0.0060
8	71.1476	4.1097	767.9458	6.4023	38.3973	0.0030
9	75.5409	9.0639	166.5397	34.9838	8.3270	0.0850
10	72.2864	8.1862	425.6133	29.9202	21.2807	0.0240
11	71.5168	6.1366	44.4236	18.0959	0.8223	0.0010
12	71.6981	7.4293	478.6601	25.5535	23.9330	0.0120
13	75.3133	8.0158	229.9234	28.9374	11.4962	0.0300
14	52.1715	7.9158	628.4500	28.3605	31.4225	0.0020
15	77.2959	6.0914	553.0234	17.8349	27.6512	0.0070
16	59.2101	8.4021	260.5900	31.1662	13.0295	0.0470
17	50.3647	26.3587	286.2332	0	14.3117	0.0010
18	60.5412	8.7268	947.0235	33.0391	47.3512	0.0010
19	64.8231	8.2218	389.9325	30.1259	19.4966	0.0410
20	70.3866	7.0882	0	23.5857	0	0.5000
21	60.9250	9.7267	695.3776	38.8080	34.7689	0.0040
22	74.6813	11.1070	306.4403	46.7711	15.3220	0.0920
23	95.4387	14.3197	391.9149	65.3059	19.5957	0.0010
24	74.4070	9.9814	663.5610	40.2772	33.1781	0.0010
25	100.7550	2.2230	288.3461	0	14.4173	0.0010

TABLE 3. Power parameter limits, initial voltages and coefficient costs for IEEE-30 network, taken from [25], [36], [38], and [39].

G	V	P^{NG}_{max}	Q^{NG}_{max}	P^{NG}_{min}	Q^{NG}_{min}	d_w	h_e	a	b	c	d	e	Prohibited zones
1	1.05	200	150	50	-20	-	-	0.00	2.00	0.00375	18	0.037	[55–66], [80–120]
2	1.04	80	60	20	-20	-	-	0.00	1.75	0.01750	16	0.038	[21–24], [45–55]
5	1.01	P_w	35	0	-30	1.6	-	-	-	-	-	-	[30–36]
8	1.01	P_s	25	0	-20	-	1.6	-	-	-	-	-	[25–30]
11	1.05	30	40	10	-10	-	-	0.00	3.00	0.02500	13	0.042	[25–28]
13	1.05	40	44.7	12	-15	-	-	0.00	3.00	0.02500	13.5	0.041	[24–30]

TABLE 4. Load power parameters for IEEE-30 network, taken from [36].

Bus	P	Q	Bus	P	Q
1	0.000	0.000	16	0.035	0.018
2	0.217	0.127	17	0.090	0.058
3	0.024	0.012	18	0.032	0.009
4	0.076	0.016	19	0.095	0.034
5	0.942	0.190	20	0.022	0.007
6	0.000	0.000	21	0.175	0.112
7	0.228	0.109	22	0.000	0.000
8	0.300	0.300	23	0.032	0.016
9	0.000	0.000	24	0.087	0.067
10	0.058	0.020	25	0.000	0.000
11	0.000	0.000	26	0.035	0.023
12	0.112	0.075	27	0.000	0.000
13	0.000	0.000	28	0.000	0.000
14	0.062	0.016	29	0.024	0.009
15	0.082	0.025	30	0.106	0.019

(positions 2,5,8,11, and 13). The second column shows the initial voltages. Columns 3 and 4 are the maximum allowed limits for P^{NG}_{max} and Q^{NG}_{max}, and columns 5 and 6 are the minimum ones P^{NG}_{min} and Q^{NG}_{min}. Columns 7 and 8 show the coefficient values for the wind and solar sources, respectively. Columns 9, 10, and 11 show the coefficients' values in computing the power from thermal sources. Columns 12 and 13 show the coefficients that help to compute $f_2(x, u)$ (valve point effect), and column 14 shows the range of prohibited zones. Thermal coefficients for buses 5 and 8 are omitted because thermal sources do not power them. Additionally, the limits for buses 5 and 8 when computing P^{NG}_{max} are set by the values obtained in Table 2 from columns 5 and 6, respectively.

Table 4 shows the active and reactive power P and Q for each bus presented in the IEEE-30 network. To include RES, each P is multiplied by the load p_d (see Table 2, column 2), and Q is left "as it is". The impedance and admittance parameters for each bus can be found in [36]. The parameters for each transformer are line 11, 1.078,0; line 12, 1.069,0; line 15, 1.032,0; and line 36, 1.068,0.

Finally, Table 5 shows the power limits for each line, taken from [46].

We developed our implementations for DEA and DEAB; AGDEA was adapted to this problem from the source code found in https://sites.google.com/view/optimization-project/files; the implementations for PSO, BBO, ABC, and NSGA-II were downloaded from www.yarpiz.com [47] and adapted to solve the OPF with the objective functions described in this article. To display the results, bold fonts remark the best metaheuristic when computing the mean of all the tests performed for each objective function and

TABLE 5. Power limit parameters for IEEE-30 network, taken from Vo et al. [46].

l	1	2	3	4	5	6	7	8	9	10	11	12	13	14	15	16	17	18	19	20	21
s_l^{max}	130	130	65	130	130	65	90	70	130	32	65	32	65	65	65	65	32	32	32	16	16
l	22	23	24	25	26	27	28	29	30	31	32	33	34	35	36	37	38	39	40	41	-
S_l^{max}	16	16	32	32	32	32	32	32	16	16	16	16	16	16	65	16	16	16	32	32	-

TABLE 6. Rate of successful cases for each tested metaheuristic algorithm with $f_1(x)$ and $f_2(x)$.

	$f_1(x)$							$f_2(x)$						
Scenario	A	B	C	D	E	F	G	A	B	C	D	E	F	G
01	100	100	100	96	100	100	100	100	100	100	95	100	100	100
02	100	100	100	97	100	100	100	98	100	100	83	2	99	100
03	100	100	100	94	100	100	100	100	100	100	86	100	100	100
04	100	100	100	96	100	100	100	100	100	100	91	100	100	100
05	100	100	100	94	100	100	100	98	93	100	90	100	100	100
06	97	100	100	94	100	100	100	99	100	100	89	100	100	100
07	100	100	100	89	100	100	100	99	93	100	91	100	100	100
08	100	100	100	94	100	100	100	97	100	100	90	99	100	100
09	100	100	100	96	100	100	100	100	100	100	93	100	100	100
10	100	100	100	95	100	100	100	97	100	100	90	8	100	100
11	100	100	100	93	100	100	100	100	100	100	91	100	100	100
12	100	100	100	92	100	100	100	100	100	100	91	2	99	100
13	100	100	100	95	100	100	100	100	100	100	93	100	100	100
14	0	1	0	0	0	0	0	0	0	0	0	0	0	0
15	100	100	100	94	100	100	100	100	100	100	90	100	99	100
16	100	100	100	93	100	100	100	96	100	100	89	100	100	100
17	100	100	100	98	100	100	100	99	100	100	98	100	100	100
18	97	98	99	39	100	100	100	95	76	99	72	100	100	97
19	100	100	100	94	100	100	100	14	45	88	4	100	73	86
20	100	100	100	99	**100**	**100**	**100**	100	100	**100**	93	100	100	100
21	100	100	100	89	100	100	100	100	100	100	88	100	100	100
22	100	100	100	92	100	100	100	98	100	100	89	4	67	100
23	100	100	100	95	100	100	100	100	100	100	94	100	100	100
24	100	100	100	90	100	100	100	0	2	0	0	31	9	2
25	0	0	0	0	0	0	0	98	99	100	93	100	100	100
CSR	2294	2299	2299	2108	**2300**	**2300**	**2300**	2188	2208	**2287**	1983	1946	2246	2285

each scenario in Table 2. For simplicity, each algorithm is identified by a capital letter as follows:

A ⤖ ABC. [13]
B ⤖ AGDEA [43]
C ⤖ DEAB Eq. 28.
D ⤖ DEA Eq. 27.
E ⤖ BBO. [12]
F ⤖ PSO. [11]
G ⤖ NSGA-II. [14]

The parameterization for each metaheuristic algorithm is listed as follows:

- Each algorithm and objective function are evaluated 100 times for each scenario listed in Table 2.
- The dimension of a solution $\mathbf{x}$ is $D = 24$.
- The number of generations is $\hat{G} = 500$, and population size is $Np = 100$.
- The validation process is applied for $\mathbf{x}^i$. For $\mathbf{u}$, the penalization factors are applied to mitigate them when solving the objective functions.
- The penalization factors applied to the objective function from [48] are: $\lambda_P = 100$, $\lambda_V = 100000$, $\lambda_Q = 100$, $\lambda_S = 100$.
- Capacitors values are equal to zero, i.e., in the buses 10 and 24 $C_{10} = 0$ and $C_{24} = 0$.
- For the shunts placed at buses 10, 12, 15, 17, 20, 21, 23, 24, 29, the operation limits are $q_{min} = 0$ and $q_{max} = 5$, i.e., $0 \leq q_i \leq 5.0$.
- For the transformers, the operation limits are $t_{min} = 0.9$ and $t_{max} = 1.1$, i.e., $0.9 \leq t_k \leq 1.1$
- For all the voltages in the buses, $v_{min} = 0.95$ and $v_{max} = 1.10$, i.e. $0.95 \leq v_m \leq 1.10$.

VI. RESULTS AND DISCUSSION

Table 6 shows how the metaheuristic algorithms behave in terms of success rate (%) when evaluating $f_1(x)$ and $f_2(x)$. Each case is tested 100 times to compute the success rate (%). BBO, PSO, and NSGA-II have the largest cumulative success rate (CSR) for $f_1(x)$ (2300), and DEAB has the largest CSR for $f_2(x)$ (2287). The worst cases are for DEA when evaluating $f_1(x)$ (2108) and BBO when evaluating $f_2(x)$ (1946). Special attention deserves scenarios 14 and 25, where the SR is almost null (just one success for AGDEA) for both functions. Also, scenario 25 is not successful at all when evaluating $f_1(x)$ (no success when using all the metaheuristic algorithms), and scenario 24 has a low percentage of success when evaluating $f_2(x)$ (with a maximum success rate of

TABLE 7. Ranking sorting values for mean (μ), for each tested metaheuristic algorithm with $f_1(x)$ and $f_2(x)$.

f(x)	$f_1(x)$							$f_2(x)$						
Sc.	A	B	C	D	E	F	G	A	B	C	D	E	F	G
01	4	6	2	5	3	1	7	3	4	1	6	2	5	7
02	4	6	3	5	2	1	7	4	5	1	7	3	2	6
03	4	5	3	6	2	1	7	4	5	3	7	2	1	6
04	4	5	3	6	2	1	7	4	5	3	7	2	1	6
05	4	5	2	7	3	1	6	4	5	2	7	3	1	6
06	4	5	2	7	3	1	6	4	5	2	7	3	1	6
07	4	5	2	7	3	1	6	4	5	2	7	3	1	6
08	4	5	3	6	2	1	7	4	5	1	7	3	2	6
09	4	5	3	7	2	1	6	4	5	3	7	2	1	6
10	4	5	3	7	2	1	6	5	4	1	7	3	2	6
11	4	7	3	6	2	1	5	4	5	3	6	2	1	7
12	4	5	3	7	2	1	6	5	4	1	7	3	2	6
13	4	5	3	7	2	1	6	4	5	2	7	1	3	6
14	7	1	7	7	7	7	7	7	7	7	7	7	7	7
15	4	5	3	6	2	1	7	3	5	2	7	1	4	6
16	4	5	2	7	3	1	6	3	4	1	7	2	5	6
17	4	6	2	5	3	1	7	4	5	2	6	3	1	7
18	4	6	2	7	3	1	5	4	5	2	7	3	1	6
19	4	5	3	7	2	1	6	4	5	2	6	3	1	7
20	4	6	3	5	2	**1**	7	3	5	2	7	**1**	4	6
21	4	5	2	7	3	1	6	3	4	1	7	2	5	6
22	4	5	3	7	2	1	6	6	4	2	7	3	1	5
23	4	6	3	7	2	1	5	4	5	3	7	2	1	6
24	4	5	3	7	2	1	6	7	2	7	7	1	3	4
25	7	7	7	7	7	7	7	4	5	2	6	3	1	7
CR	106	131	75	162	68	**37**	157	105	118	58	170	63	**57**	153

TABLE 8. Minimum (m) values for each tested metaheuristic algorithm with $f_1(x)$ and $f_2(x)$.

f(x)	$f_1(x)$							$f_2(x)$						
Sc.	A	B	C	D	E	F	G	A	B	C	D	E	F	G
01	5	4	2	6	3	1	7	5	4	1	7	2	3	6
02	4	5	3	7	2	1	6	5	3	2	6	4	1	7
03	5	4	3	7	1	2	6	5	4	3	7	2	1	6
04	5	4	3	7	2	1	6	5	4	3	7	2	1	6
05	5	4	2	7	3	1	6	5	4	2	7	3	1	6
06	5	4	3	7	2	1	6	5	4	3	7	2	1	6
07	6	4	3	7	2	1	5	5	4	2	7	3	1	6
08	5	4	3	7	2	1	6	5	4	2	7	3	1	6
09	5	4	3	7	1	2	6	5	4	3	7	2	1	6
10	5	4	3	7	2	1	6	6	4	2	7	3	1	5
11	5	4	3	7	1	2	6	5	4	3	7	2	1	6
12	5	4	3	7	2	1	6	6	4	2	7	3	1	5
13	5	4	3	7	1	2	6	5	3	4	7	2	1	6
14	7	1	7	7	7	7	7	7	7	7	7	7	7	7
15	5	4	3	7	1	2	6	5	4	2	7	1	3	6
16	5	4	3	7	2	1	6	5	3	2	7	1	4	6
17	5	4	3	6	2	1	7	5	4	2	6	3	1	7
18	5	4	2	7	3	1	6	5	4	2	7	3	1	6
19	5	4	3	7	2	1	6	5	4	3	7	2	1	6
20	5	4	3	6	**1**	2	7	5	3	2	7	**1**	4	6
21	5	4	2	7	3	1	6	5	4	1	7	2	3	6
22	5	4	3	7	1	2	6	6	3	2	7	4	1	5
23	5	4	3	7	2	1	6	5	4	3	7	2	1	6
24	5	4	3	7	2	1	6	7	3	7	7	2	1	4
25	7	7	7	7	7	7	7	5	4	2	7	3	1	6
CR	129	101	79	172	57	**44**	154	132	97	67	173	64	**43**	148

31 % when using BBO). That means the penalization factor did not vanish when the objective function was solved. According to Table 2, scenario 20 is the most representative because it has a probability of 0.5, being DEA the worst metaheuristic algorithm (93 % success rate).

Table 7 shows the ranking for each metaheuristic algorithm when using the mean (μ) as a criterion, with 1 being the best and 7 the worst. Obtaining the cumulative ranking (CR), PSO is the best among all the available metaheuristic algorithms for both functions, 37 for $f_1(x)$ and 57 for $f_2(x)$, respectively. A note should be made for cases 14 and 24

TABLE 9. Maximum (*M*) values for each tested metaheuristic algorithm with $f_1(x)$ and $f_2(x)$.

f(x)	$f_1(x)$							$f_2(x)$						
Sc.	A	B	C	D	E	F	G	A	B	C	D	E	F	G
01	4	7	2	5	3	1	6	3	7	1	4	2	5	6
02	4	7	3	5	2	1	6	4	5	1	7	3	2	6
03	4	7	3	5	2	1	6	4	6	3	7	2	1	5
04	4	7	3	5	2	1	6	4	7	3	6	2	1	5
05	4	6	2	7	3	1	5	4	7	2	6	3	1	5
06	4	7	2	6	3	1	5	4	6	2	7	3	1	5
07	4	6	2	7	3	1	5	4	5	2	7	3	1	6
08	4	7	2	6	3	1	5	4	5	2	7	3	1	6
09	4	7	3	5	2	1	6	4	7	3	6	2	1	5
10	4	7	3	5	2	1	6	4	5	2	7	3	1	6
11	4	7	3	5	2	1	6	4	7	3	5	2	1	6
12	4	7	3	5	2	1	6	4	5	1	7	3	2	6
13	4	7	3	5	2	1	6	3	7	2	5	1	4	6
14	7	1	7	7	7	7	7	7	7	7	7	7	7	7
15	4	7	3	5	2	1	6	3	7	2	5	1	6	4
16	4	6	2	7	3	1	5	2	3	1	5	6	4	7
17	4	7	2	5	3	1	6	4	6	2	5	3	1	7
18	4	7	2	6	3	1	5	4	7	2	6	3	1	5
19	4	6	2	7	3	1	5	4	5	2	6	3	1	7
20	4	7	2	5	3	**1**	6	3	7	2	4	**1**	5	6
21	4	6	2	7	3	1	5	3	5	1	7	2	6	4
22	4	7	2	6	3	1	5	6	4	2	7	3	1	5
23	4	7	3	6	2	1	5	4	6	2	7	3	1	5
24	4	7	2	6	3	1	5	7	2	7	7	1	4	3
25	7	7	7	7	7	7	7	4	6	2	5	3	1	7
CR	106	164	70	145	73	**37**	141	101	144	**59**	152	68	60	140

TABLE 10. Summary of score ranking for (μ), minimum (*m*), and maximum (*M*) for all the tested objective functions and metaheuristic algorithms.

Function	Feature	ABC	AGDEA	DEAB	DEA	BBO	PSO	NSGA-II
$f_1(x)$	μ	106	131	75	162	68	**37**	157
	m	129	101	79	172	57	**44**	154
	M	106	164	70	145	73	**37**	141
	CSR	2294	2299	2299	2108	**2300**	**2300**	**2300**
	μ (0.5)	4	6	3	5	2	**1**	7
	m (0.5)	5	4	3	6	**1**	2	7
	M (0.5)	4	7	2	5	3	**1**	6
	SR (0.5)	100	100	100	99	100	**100**	100
$f_2(x)$	μ	105	118	58	170	63	**57**	153
	m	132	97	67	173	64	**43**	148
	M	101	144	**59**	152	68	60	140
	CSR	2188	2208	**2287**	1983	1946	2246	2285
	μ (0.5)	3	5	2	7	**1**	4	6
	m (0.5)	5	3	2	7	**1**	4	6
	M (0.5)	3	7	2	4	**1**	5	6
	SR (0.5)	100	100	100	93	**100**	100	100

TABLE 11. Summary of weighted cumulative rating (WCR) and weighted cumulative successful rate (WCSR) for (μ), minimum (*m*) and maximum (*M*) for all the tested objective functions and metaheuristic algorithms.

Function	Feature	ABC	AGDEA	DEAB	DEA	BBO	PSO	NSGA-II
$f_1(x)$	μ (WCSR)	4.0090	5.5040	2.9460	5.8470	2.0810	**1.0180**	6.6460
	m (WCSR)	5.0080	4.0010	3.0020	6.4980	**1.2500**	1.7930	6.4990
	M (WCSR)	4.0090	6.8860	2.3090	5.3100	2.7180	**1.0180**	5.8010
	WCR	99.6910	99.6990	99.6990	96.2360	**99.7000**	**99.7000**	**99.7000**
$f_2(x)$	μ (WCSR)	3.6700	4.8210	**2.1370**	6.9550	**1.6630**	2.8460	5.9530
	m (WCSR)	5.1340	3.3320	**2.3300**	6.9950	**1.7000**	2.6770	5.8770
	M (WCSR)	3.5570	6.2780	**2.1630**	5.1220	**1.8520**	3.3210	5.7520
	WCR	95.6890	97.3520	**99.2070**	87.7230	87.1200	95.5430	99.1250

(for $f_2(x)$) and 25 (for $f_1(x)$), where the worst ranking is assigned (7) due to a lack of success of the tested algorithms. The worst case is for DEA, 162 for $f_1(x)$ and 170 for $f_2(x)$, respectively. For the special scenario (scenario 20), PSO is still the best for $f_1(x)$, but for $f_2(x)$, the best is BBO.

Table 8 shows the ranking for each metaheuristic algorithm when using the minimum value (m) as a criterion. Obtaining

TABLE 12. Mean (μ) values for each tested metaheuristic algorithm with $f_1(x)$.

Sc.	ABC	AGDEA	DEAB	DEA	BBO	PSO	NSGA-II
01	374.8166	375.2178	374.6601	375.0363	374.6624	374.6578	375.2903
02	441.1928	441.7818	441.0842	441.7417	441.0819	441.0796	441.8581
03	471.5775	472.1126	471.4751	472.2198	471.4717	471.4698	472.2414
04	468.3828	468.9414	468.3107	469.0102	468.3073	468.3058	469.0509
05	369.9769	370.0452	369.7131	370.3623	369.7851	369.7079	370.1354
06	456.0311	456.2058	455.7736	456.6157	455.8387	455.7668	456.2422
07	383.0392	383.1402	382.7806	383.5535	382.8530	382.7751	383.2005
08	473.2229	473.7376	473.1152	473.8578	473.1126	473.1099	473.8660
09	511.4092	511.9122	511.3217	512.0875	511.3173	511.3157	512.0478
10	473.1413	473.5092	472.9917	473.8032	472.9886	472.9860	473.7354
11	512.8408	513.4803	512.7930	513.3915	512.7893	512.7883	513.3887
12	470.6330	471.0839	470.4879	471.3030	470.4848	470.4824	471.2233
13	513.6858	514.2992	513.6094	514.4100	513.6048	513.6034	514.3451
14	Inf	315.3528	Inf	Inf	Inf	Inf	Inf
15	524.0086	524.7262	523.9351	524.7284	523.9300	523.9288	524.7314
16	377.7176	377.9008	377.4714	378.1902	377.4814	377.4666	378.0121
17	343.2888	343.5879	343.1316	343.4721	343.1327	343.1298	343.7458
18	353.1096	353.3127	352.8649	353.7278	352.9927	352.8562	353.2017
19	415.0088	415.2803	414.7958	415.5618	414.7946	414.7903	415.4060
20	495.6023	496.1635	495.5661	495.9706	495.5644	495.5636	496.2144
21	361.3857	361.4297	361.1408	361.9407	361.2592	361.1345	361.4979
22	478.5973	479.0081	478.4173	479.2275	478.4142	478.4114	479.1234
23	624.1751	624.8169	624.1091	625.0136	624.1019	624.1007	624.7703
24	462.5707	462.8961	462.3548	463.1728	462.3529	462.3487	463.0154
25	Inf	Inf	Inf	Inf	Inf	Inf	Inf

TABLE 13. Minimum (m) values for each tested metaheuristic algorithm with $f_1(x)$.

Sc.	ABC	AGDEA	DEAB	DEA	BBO	PSO	NSGA-II
01	374.7568	374.6731	374.6586	374.9112	374.6586	374.6578	375.1073
02	441.1438	441.1898	441.0816	441.5667	441.0798	441.0796	441.4807
03	471.5321	471.4825	471.4716	472.0077	471.4698	471.4698	471.8135
04	468.3508	468.3105	468.3076	468.7918	468.3061	468.3058	468.6040
05	369.8704	369.7250	369.7096	370.1313	369.7106	369.7079	369.9690
06	455.9383	455.8405	455.7698	456.3095	455.7684	455.7668	455.9921
07	382.9637	382.9006	382.7777	383.3198	382.7764	382.7751	382.9500
08	473.1650	473.1545	473.1122	473.6060	473.1100	473.1099	473.5054
09	511.3699	511.3255	511.3180	511.8475	511.3157	511.3157	511.6896
10	473.0789	473.0037	472.9878	473.5881	472.9861	472.9860	473.3385
11	512.8251	512.7966	512.7900	513.1437	512.7883	512.7883	512.8840
12	470.5664	470.5129	470.4845	471.0911	470.4825	470.4824	470.8664
13	513.6525	513.6179	513.6061	514.0046	513.6034	513.6034	513.8679
14	Inf	315.3528	Inf	Inf	Inf	Inf	Inf
15	523.9767	523.9335	523.9316	524.4675	523.9288	523.9288	524.3157
16	377.6398	377.5345	377.4689	377.9641	377.4676	377.4666	377.8274
17	343.2140	343.1507	343.1305	343.3612	343.1299	343.1298	343.4279
18	353.0599	352.9863	352.8593	353.4760	352.9041	352.8562	353.0905
19	414.8865	414.8216	414.7924	415.3233	414.7904	414.7903	415.2215
20	495.5878	495.5700	495.5644	495.8382	495.5636	495.5636	495.8614
21	361.2852	361.1574	361.1370	361.6630	361.1558	361.1345	361.3950
22	478.5452	478.4256	478.4136	478.9571	478.4114	478.4114	478.8046
23	624.1499	624.1179	624.1034	624.7987	624.1008	624.1007	624.2903
24	462.4849	462.3662	462.3510	462.8217	462.3488	462.3487	462.8095
25	Inf	Inf	Inf	Inf	Inf	Inf	Inf

the cumulative ranking (CR), again, PSO is the best among all the available metaheuristic algorithms for both functions 44 for $f_1(x)$ and 43 for $f_2(x)$, respectively. The worst case is obtained for DEA, 172 for $f_1(x)$ and 173 for $f_2(x)$, respectively. For the special scenario (scenario 20), BBO is the best for $f_1(x)$ and $f_2(x)$.

Table 9 shows the ranking for each metaheuristic algorithm when using the maximum value (M) as a criterion. Obtaining the cumulative ranking (CR), again, PSO is the best but just for $f_1(x)$ (37); meanwhile, DEAB is the best for $f_2(x)$ (59). The worst case is obtained for AGDEA when evaluating $f_1(x)$ (164) and DEA when evaluating $f_2(x)$ (152). For the special scenario (scenario 20), PSO is the best for $f_1(x)$ and BBO is the best for $f_2(x)$.

A. DISCUSSION

When using the cumulative success rate as the criterion to classify the algorithms, BBO, PSO, and NSGA-II are

TABLE 14. Maximum (M) values for each tested metaheuristic algorithm with $f_1(x)$.

Sc.	ABC	AGDEA	DEAB	DEA	BBO	PSO	NSGA-II
01	374.9426	384.3407	374.6630	375.2199	374.6709	374.6578	375.5805
02	441.2434	442.6553	441.0954	441.9493	441.0853	441.0796	442.2212
03	471.6548	472.9567	471.4816	472.4532	471.4752	471.4698	472.6723
04	468.4500	469.7121	468.3149	469.1910	468.3108	468.3058	469.5205
05	370.0668	370.4285	369.7183	370.5987	369.9293	369.7079	370.3871
06	456.1248	458.7442	455.7799	456.8319	455.9914	455.7668	456.4269
07	383.1322	383.5193	382.7867	383.8989	382.9669	382.7751	383.2885
08	473.3391	474.4004	473.1194	474.1967	473.1212	473.1099	474.1592
09	511.4819	512.9675	511.3265	512.3910	511.3241	511.3157	512.4618
10	473.2140	474.2966	472.9982	474.1145	472.9943	472.9860	474.1250
11	512.8732	514.4519	512.7992	513.5577	512.7923	512.7883	513.8270
12	470.7342	472.4543	470.4939	471.5963	470.4924	470.4824	471.6006
13	513.7664	515.2851	513.6168	514.7429	513.6104	513.6034	514.9472
14	Inf	315.3528	Inf	Inf	Inf	Inf	Inf
15	524.0579	525.5432	523.9421	525.0331	523.9340	523.9288	525.1221
16	377.8757	378.3069	377.4773	378.4414	377.5887	377.4666	378.2370
17	343.3527	344.1912	343.1336	343.5772	343.1431	343.1298	343.9981
18	353.1584	363.6120	352.8725	353.9714	353.0954	352.8562	353.3641
19	415.1025	415.7145	414.8018	415.7976	414.8057	414.7903	415.6969
20	495.6177	497.0390	495.5681	496.0775	495.5691	495.5636	496.7486
21	361.4618	361.6459	361.1518	362.2326	361.3688	361.1345	361.6168
22	478.6839	479.5329	478.4230	479.5049	478.4266	478.4114	479.3761
23	624.2170	625.9267	624.1182	625.3188	624.1078	624.1007	625.2306
24	462.6964	464.4801	462.3618	463.4218	462.3627	462.3487	463.2480
25	Inf	Inf	Inf	Inf	Inf	Inf	Inf

TABLE 15. Mean (μ) values for each tested metaheuristic algorithm with $f_2(x)$.

Sc.	ABC	AGDEA	DEAB	DEA	BBO	PSO	NSGA-II
01	393.0262	393.4247	392.7913	393.4676	392.7975	393.4346	393.6423
02	458.7565	458.7759	458.2745	459.1062	458.3904	458.2983	459.0302
03	480.9152	481.3503	480.8037	481.8083	480.7969	480.7934	481.5889
04	474.3871	474.8843	474.3062	475.2304	474.3004	474.2972	475.0304
05	380.6120	380.7058	380.2552	381.2880	380.4057	380.2461	380.8568
06	471.1350	471.2453	470.7919	472.2165	470.9297	470.7772	471.4153
07	395.3326	395.4220	394.9901	396.2057	395.1373	394.9808	395.5817
08	487.7567	487.8399	487.3169	488.2295	487.4290	487.3253	488.0690
09	517.2421	517.6654	517.1394	518.2319	517.1305	517.1278	517.9104
10	492.5190	492.3786	491.8788	492.9320	492.0356	491.8851	492.5544
11	520.4223	521.0317	520.3201	521.2441	520.3194	520.3121	521.3027
12	489.8951	489.8047	489.2593	490.3064	489.3805	489.2787	489.9673
13	518.6236	519.1997	518.4777	519.7543	518.4754	518.4837	519.5444
14	Inf	Inf	Inf	Inf	Inf	Inf	Inf
15	529.2434	530.1186	529.1099	530.5391	529.1046	529.2935	530.2125
16	396.2115	396.3723	395.8861	397.0432	395.9866	396.5884	396.6676
17	364.8446	365.1028	364.5030	365.1501	364.5148	364.4951	366.1773
18	353.4216	353.5349	353.0769	354.4568	353.2962	353.0650	353.5439
19	440.9170	440.9397	440.2647	442.6693	440.3171	440.2207	442.8915
20	501.2904	501.7317	501.2320	502.0238	501.2318	501.6366	501.9879
21	366.9999	367.0461	366.6689	367.9803	366.8643	367.1061	367.1446
22	503.3987	503.1573	502.6922	503.9177	502.8569	502.6738	503.3414
23	632.4700	633.1216	632.3290	633.7861	632.3275	632.3146	633.4398
24	Inf	491.4160	Inf	Inf	490.6776	491.7559	493.6502
25	846.9450	847.2301	846.5655	847.8113	846.6199	846.5092	849.6284

successful algorithms for $f_1(x)$ (CSR of 2300 for the three algorithms) and DEAB is successful for $f_2(2)$ (CSR of 2287). However, the discriminant rate (DR) is needed to contrast these results and see how to classify which algorithm results the best among all those evaluated. When DR is considered, PSO is the best when applied μ and minimum value m classification criteria for both functions (37 and 44 for $f_1(x)$, 57 and 43 for $f_2(x)$), but DEAB is the best when evaluating $f_2(x)$ for maximum value M classification criterion, and PSO is the best when evaluating $f_1(X)$ (value 37). Additionally, it is useful to consider how each algorithm behaves in scenario 20 because it appears with a probability of 0.5. When using the μ criterion, PSO is the best for $f_1(x)$, and BBO is the best for $f_2(x)$. When using m criterion, BBO is the best for $f_1(x)$ and $f_2(x)$. When using M, PSO is the best for $f_1(x)$ and BBO is the best for $f_2(x)$. Table 6 shows that DEA has the worst success rate (SR) performance when evaluating scenario 20. These results are summarized in Table 10.

TABLE 16. Minimum (m) values for each tested metaheuristic algorithm with $f_2(x)$.

Sc.	ABC	AGDEA	DEAB	DEA	BBO	PSO	NSGA-II
01	392.9341	392.8401	392.7882	393.2830	392.7890	392.7926	393.2340
02	458.6093	458.2980	458.2632	458.7179	458.3085	458.2616	458.7266
03	480.8725	480.8007	480.7980	481.4116	480.7939	480.7934	481.0720
04	474.3511	474.3077	474.2999	474.8739	474.2976	474.2972	474.6735
05	380.4287	380.3647	380.2492	380.9261	380.2575	380.2461	380.5715
06	471.0024	470.8247	470.7835	471.5194	470.7800	470.7772	471.2117
07	395.1961	395.0154	394.9845	395.7778	394.9868	394.9808	395.3554
08	487.5832	487.3627	487.3049	487.8670	487.3231	487.2961	487.6190
09	517.1996	517.1450	517.1327	517.8886	517.1279	517.1278	517.5006
10	492.3274	491.9369	491.8654	492.4046	491.8947	491.8560	492.1703
11	520.3788	520.3375	520.3155	520.9429	520.3132	520.3121	520.7404
12	489.6905	489.3538	489.2483	489.8391	489.3308	489.2377	489.6648
13	518.5525	518.4705	518.4714	519.3925	518.4685	518.4672	518.6343
14	Inf	Inf	Inf	Inf	Inf	Inf	Inf
15	529.1868	529.1576	529.1024	530.0275	529.0976	529.1158	529.3150
16	396.1012	395.9203	395.8802	396.6399	395.8791	396.0795	396.2824
17	364.7057	364.5390	364.4977	364.8744	364.5001	364.4951	365.0232
18	353.3448	353.1832	353.0697	353.8173	353.1583	353.0650	353.3656
19	440.6345	440.2730	440.2355	442.4486	440.2239	440.2207	441.0245
20	501.2666	501.2313	501.2287	501.7834	501.2274	501.2364	501.3903
21	366.9070	366.8112	366.6603	367.4195	366.7264	366.7666	366.9095
22	503.0734	502.7178	502.6770	503.3494	502.7874	502.6698	502.7969
23	632.4017	632.3369	632.3188	633.3112	632.3155	632.3146	632.9133
24	Inf	491.3270	Inf	Inf	490.5607	490.5460	493.6244
25	846.7807	846.6317	846.5387	847.4815	846.5412	846.5083	846.9156

TABLE 17. Maximum (M) values for each tested metaheuristic algorithm with $f_2(x)$.

Sc.	ABC	AGDEA	DEAB	DEA	BBO	PSO	NSGA-II
01	393.1451	397.5299	392.7991	393.7286	392.8098	393.9958	394.0039
02	458.8998	459.2849	458.3054	459.3832	458.4723	458.3407	459.3579
03	480.9847	482.2063	480.8177	482.2156	480.8039	480.7934	482.0285
04	474.4465	475.8900	474.3140	475.5217	474.3071	474.2972	475.3465
05	380.7222	382.0110	380.2690	381.6945	380.5473	380.2461	381.1555
06	471.2576	472.6303	470.8057	472.8030	471.0892	470.7772	471.6635
07	395.4345	395.7311	394.9998	396.6889	395.3990	394.9808	395.7450
08	487.9529	488.3412	487.3658	488.6422	487.6512	487.3453	488.4079
09	517.3285	519.3376	517.1500	518.7628	517.1370	517.1278	518.1910
10	492.6536	492.8150	491.9544	493.3049	492.1620	491.9214	492.8469
11	520.4782	522.1004	520.3295	521.5160	520.3293	520.3121	522.0801
12	490.0608	490.3100	489.2883	490.6172	489.4302	489.3268	490.3564
13	518.7531	520.3651	518.4855	520.1537	518.4846	520.1120	520.2468
14	Inf	Inf	Inf	Inf	Inf	Inf	Inf
15	529.3198	531.6582	529.1216	531.0089	529.1205	531.5174	530.9399
16	396.3457	396.7621	395.8971	397.4047	398.2950	397.0539	399.7943
17	365.1558	365.7621	364.5109	365.3773	364.6210	364.4951	368.7287
18	353.4949	362.2123	353.0917	354.8708	353.4336	353.0650	353.7014
19	441.1091	442.4051	440.3651	442.9440	440.6128	440.2207	445.8662
20	501.3372	502.8832	501.2385	502.3514	501.2380	502.3836	502.4892
21	367.0542	367.3599	366.6838	368.6031	367.0103	367.5217	367.3435
22	503.6269	503.5934	502.7120	504.7163	502.9302	502.6865	503.6043
23	632.5540	634.2151	632.3485	634.2763	632.3556	632.3146	634.0516
24	Inf	491.5051	Inf	Inf	490.8548	501.4350	493.6760
25	847.1592	850.2777	846.5960	848.2686	846.9734	846.5180	854.8164

Another approach that can be useful to determine which algorithm has the best performance considers the use of the probability of each case as a weight, as proposed in [25]. For instance, all the row elements of Table 6, Table 7, Table 8 and Table 9 corresponding to scenario 1 should be multiplied by the probability value corresponding to scenario 1 (see column 7 of Table 2), and so on with the rest of the row elements with the respective probability value (e.g., row elements of scenario 2 multiplied by the probability value of scenario 2, etc.). In the end, the summation of results is applied in a similar way to the additions shown in Table 6, Table 7, Table 8, and Table 9. Then, Table 11 shows the summation of the results obtained with this approach. In terms of weighted CSR (WCSR), the results remain the same, DEAB is the best for $f_2(x)$; BBO, PSO, and NSGA-II are the best for $f_1(x)$. Nevertheless, with weighted CR (WCR), BBO presents advantages when evaluating $f_1(x)$ with m criterion and $f_2(x)$ with μ, m, and M criteria; meanwhile, PSO presents advantages when evaluating $f_1(x)$ with μ and M criteria. These results contrast when evaluated without weight because now BBO is better than PSO for most of the used criteria for $f_1(x)$ and $f_2(x)$. But BBO has the worst WCR when evaluating $f_2(x)$, so the best choice, in this case, is DEAB because it has the largest WRC and the second-best WCRS for all the criteria μ, m, and M.

VII. CONCLUSION AND FUTURE WORK

Renewable energy sources pose the most challenging conditions in solving the OPF. In this work, we have addressed their stochastic behavior using existing approaches found in the literature. The authors have shown that the inclusion of RES in a stochastic way can be successfully analyzed from typical scenarios of costs (i.e., $f_1(x)$) to hard scenarios like the cost function with valve-point effect and prohibited zones (i.e., $f_2(x)$). Metaheuristic algorithms were tested for 25 representative scenarios obtained from 1000 random scenarios. In terms of performance, the weighted results in Table 11, BBO, PSO, and NSGA-II were the best choices when evaluating $f_1(x)$, achieving all of them WCR values of 99.7%. Meanwhile, BBO seems to be the best option to evaluate $f_2(x)$ WCSR metrics. However, BBO presents the worst WCR value among all the tested metaheuristics for $f_2(x)$, with a value of 87.1%. Thus, DEAB should be considered a better choice for $f_2(x)$ because it presents the best WRC (99.2 %) and the second-best WCRS values for all the evaluated criteria (μ, m, and M).

Future research should focus on expanding to larger power networks like the IEEE-57 bus and IEEE-118 bus networks, employing enhanced metaheuristic algorithms to evaluate their success rates (%) and ranking metrics for the mean (μ), minimum (m), and maximum (M) outcomes. Statistical performance analysis is another addition to the work that can be explored in the future. Also, investigating the inherent uncertainties in power flow and operational dynamics, particularly concerning renewable energy integration, will provide valuable insights into enhancing system reliability and efficiency. Additionally, exploring modern approaches to system expansion planning considering new market designs [49] can be an interesting research venue since it is a new area crucial for addressing upcoming power system optimization and management challenges.

APPENDIX

The Appendix includes Tables 12-17 that summarize the mean, minimum, and maximum values for each tested scenario and each algorithm to compute the ranking sorted values shown in the Results and Discussion section.

REFERENCES

[1] M. Zastempowski, "Analysis and modeling of innovation factors to replace fossil fuels with renewable energy sources–Evidence from European union enterprises," *Renew. Sustain. Energy Rev.*, vol. 178, May 2023, Art. no. 113262.

[2] D. Dabhi and K. Pandya, "Enhanced velocity differential evolutionary particle swarm optimization for optimal scheduling of a distributed energy resources with uncertain scenarios," *IEEE Access*, vol. 8, pp. 27001–27017, 2020.

[3] V. Ruffato-Ferreira, R. da Costa Barreto, A. O. Junior, W. L. Silva, J. A. S. do Nascimento, and M. A. V. de Freitas, "A foundation for the strategic long-term planning of the renewable energy sector in Brazil: Hydroelectricity and wind energy in the face of climate change scenarios," *Renew. Sustain. Energy Rev.*, vol. 72, pp. 1124–1137, May 2017.

[4] T. D. de Lima, J. Soares, F. Lezama, J. F. Franco, and Z. Vale, "A risk-based planning approach for sustainable distribution systems considering EV charging stations and carbon taxes," *IEEE Trans. Sustain. Energy*, vol. 14, no. 4, pp. 2294–2307, Oct. 2023.

[5] J. K. Skolfield and A. R. Escobedo, "Operations research in optimal power flow: A guide to recent and emerging methodologies and applications," *Eur. J. Oper. Res.*, vol. 300, no. 2, pp. 387–404, Jul. 2022.

[6] D. Dabhi and K. Pandya, "Uncertain scenario based MicroGrid optimization via hybrid levy particle swarm variable neighborhood search optimization (HL_PS_VNSO)," *IEEE Access*, vol. 8, pp. 108782–108797, 2020.

[7] A. Ehsan and Q. Yang, "Optimal integration and planning of renewable distributed generation in the power distribution networks: A review of analytical techniques," *Appl. Energy*, vol. 210, pp. 44–59, Jan. 2018.

[8] R. S. Ferreira, C. L. T. Borges, and M. V. F. Pereira, "A flexible mixed-integer linear programming approach to the AC optimal power flow in distribution systems," *IEEE Trans. Power Syst.*, vol. 29, no. 5, pp. 2447–2459, Sep. 2014.

[9] S. Kahourzade, A. Mahmoudi, and H. B. Mokhlis, "A comparative study of multi-objective optimal power flow based on particle swarm, evolutionary programming, and genetic algorithm," *Electr. Eng.*, vol. 97, no. 1, pp. 1–12, Mar. 2015.

[10] G. Castanón, A. F. Martínez-Herrera, A. M. Sarmiento, A. Aragon-Zavala, and F. Lezama, "Comparative analysis of nature-inspired algorithms for optimal power flow problem: A focus on penalty-vanishing terms and algorithm performance," *IEEE Access*, vol. 12, pp. 29940–29958, 2024.

[11] Eberhart and Y. Shi, "Particle swarm optimization: Developments, applications and resources," in *Proc. Congr. Evol. Comput.*, vol. 1, May 2001, pp. 81–86.

[12] D. Simon, "Biogeography-based optimization," *IEEE Trans. Evol. Comput.*, vol. 12, no. 6, pp. 702–713, Dec. 2008.

[13] D. Karaboga and B. Basturk, "A powerful and efficient algorithm for numerical function optimization: Artificial bee colony (ABC) algorithm," *J. Global Optim.*, vol. 39, no. 3, pp. 459–471, Oct. 2007.

[14] K. Deb, A. Pratap, S. Agarwal, and T. Meyarivan, "A fast and elitist multiobjective genetic algorithm: NSGA-II," *IEEE Trans. Evol. Comput.*, vol. 6, no. 2, pp. 182–197, Apr. 2002.

[15] Y. Hu, Z. Bie, T. Ding, and Y. Lin, "An NSGA-II based multi-objective optimization for combined gas and electricity network expansion planning," *Appl. Energy*, vol. 167, pp. 280–293, Apr. 2016.

[16] S. M. Mohseni-Bonab, A. Rabiee, and B. Mohammadi-Ivatloo, "Voltage stability constrained multi-objective optimal reactive power dispatch under load and wind power uncertainties: A stochastic approach," *Renew. Energy*, vol. 85, pp. 598–609, Jan. 2016.

[17] L. Shi, C. Wang, L. Yao, Y. Ni, and M. Bazargan, "Optimal power flow solution incorporating wind power," *IEEE Syst. J.*, vol. 6, no. 2, pp. 233–241, Jun. 2012.

[18] U. Khaled, A. M. Eltamaly, and A. Beroual, "Optimal power flow using particle swarm optimization of renewable hybrid distributed generation," *Energies*, vol. 10, no. 7, p. 1013, Jul. 2017.

[19] S. Surender Reddy and P. R. Bijwe, "Day-ahead and real time optimal power flow considering renewable energy resources," *Int. J. Electr. Power Energy Syst.*, vol. 82, pp. 400–408, Nov. 2016.

[20] A. Maulik and D. Das, "Optimal power dispatch considering load and renewable generation uncertainties in an AC–DC hybrid microgrid," *IET Gener., Transmiss. Distribution*, vol. 13, no. 7, pp. 1164–1176, Apr. 2019.

[21] E. E. Elattar, "Optimal power flow of a power system incorporating stochastic wind power based on modified moth swarm algorithm," *IEEE Access*, vol. 7, pp. 89581–89593, 2019.

[22] E. E. Elattar and S. K. ElSayed, "Modified Jaya algorithm for optimal power flow incorporating renewable energy sources considering the cost, emission, power loss and voltage profile improvement," *Energy*, vol. 178, pp. 598–609, Jul. 2019.

[23] Y. M. Atwa and E. F. El-Saadany, "Probabilistic approach for optimal allocation of wind-based distributed generation in distribution systems," *IET Renew. Power Gener.*, vol. 5, no. 1, p. 79, 2011.

[24] N. H. Awad, M. Z. Ali, R. Mallipeddi, and P. N. Suganthan, "An efficient differential evolution algorithm for stochastic OPF based active–reactive power dispatch problem considering renewable generators," *Appl. Soft Comput.*, vol. 76, pp. 445–458, Mar. 2019.

[25] P. P. Biswas, P. N. Suganthan, R. Mallipeddi, and G. A. J. Amaratunga, "Optimal reactive power dispatch with uncertainties in load demand and renewable energy sources adopting scenario-based approach," *Appl. Soft Comput.*, vol. 75, pp. 616–632, Feb. 2019.

[26] S. Li, W. Gong, L. Wang, X. Yan, and C. Hu, "Optimal power flow by means of improved adaptive differential evolution," *Energy*, vol. 198, May 2020, Art. no. 117314.

[27] S. Li, W. Gong, L. Wang, and Q. Gu, "Multi-objective optimal power flow with stochastic wind and solar power," *Appl. Soft Comput.*, vol. 114, Jan. 2022, Art. no. 108045.

[28] E. Naderi, M. Pourakbari-Kasmaei, F. V. Cerna, and M. Lehtonen, "A novel hybrid self-adaptive heuristic algorithm to handle single- and multi-objective optimal power flow problems," *Int. J. Electr. Power Energy Syst.*, vol. 125, Feb. 2021, Art. no. 106492.

[29] J. Sarda, K. Pandya, and K. Y. Lee, "Dynamic optimal power flow with cross entropy covariance matrix adaption evolutionary strategy for systems with electric vehicles and renewable generators," *Int. J. Energy Res.*, vol. 45, no. 7, pp. 10869–10881, Jun. 2021.

[30] H. T. Kahraman, M. Akbel, and S. Duman, "Optimization of optimal power flow problem using multi-objective manta ray foraging optimizer," *Appl. Soft Comput.*, vol. 116, Feb. 2022, Art. no. 108334.

[31] M. H. Nadimi-Shahraki, A. Fatahi, H. Zamani, S. Mirjalili, and D. Oliva, "Hybridizing of whale and moth-flame optimization algorithms to solve diverse scales of optimal power flow problem," *Electronics*, vol. 11, no. 5, p. 831, Mar. 2022.

[32] A. A. Mohamed, S. Kamel, M. H. Hassan, M. I. Mosaad, and M. Aljohani, "Optimal power flow analysis based on hybrid gradient-based optimizer with moth–flame optimization algorithm considering optimal placement and sizing of FACTS/wind power," *Mathematics*, vol. 10, no. 3, p. 361, Jan. 2022.

[33] M. H. Hassan, F. Daqaq, S. Kamel, A. G. Hussien, and H. M. Zawbaa, "An enhanced hunter-prey optimization for optimal power flow with FACTS devices and wind power integration," *IET Gener., Transmiss. Distribution*, vol. 17, no. 14, pp. 3115–3139, Jul. 2023.

[34] M. H. Hassan, S. Kamel, and A. G. Hussien, "Optimal power flow analysis considering renewable energy resources uncertainty based on an improved wild horse optimizer," *IET Gener., Transmiss. Distribution*, vol. 17, no. 16, pp. 3582–3606, Aug. 2023.

[35] J. Sarda, K. Pandya, and K. Y. Lee, "Hybrid cross entropy—Cuckoo search algorithm for solving optimal power flow with renewable generators and controllable loads," *Optim. Control Appl. Methods*, vol. 44, no. 2, pp. 508–532, Mar. 2023.

[36] A. A. Abou El Ela, M. A. Abido, and S. R. Spea, "Optimal power flow using differential evolution algorithm," *Electr. Eng. (Archiv fur Elektrotechnik)*, vol. 91, no. 2, pp. 69–78, 2009.

[37] A. A. A. E. Ela, M. A. Abido, and S. R. Spea, "Differential evolution algorithm for optimal reactive power dispatch," *Electric Power Syst. Res.*, vol. 81, no. 2, pp. 458–464, Feb. 2011.

[38] T. Niknam, M. R. Narimani, and R. Azizipanah-Abarghooee, "A new hybrid algorithm for optimal power flow considering prohibited zones and valve point effect," *Energy Convers. Manage.*, vol. 58, pp. 197–206, Jun. 2012.

[39] S. Shafiq, N. Javaid, and S. Aslam, "Optimal power flow control in a smart micro-grid using bird swarm algorithm," in *Proc. 5th Int. Multi-Topic ICT Conf. (IMTIC)*, Apr. 2018, pp. 1–7.

[40] M. A. Abido, "Optimal power flow using particle swarm optimization," *Int. J. Electr. Power Energy Syst.*, vol. 24, no. 7, pp. 563–571, Oct. 2002.

[41] R. Storn and K. Price, "Differential evolution—A simple and efficient heuristic for global optimization over continuous spaces," *J. Global Optim.*, vol. 11, pp. 341–359, Dec. 1997.

[42] Sk. M. Islam, S. Das, S. Ghosh, S. Roy, and P. N. Suganthan, "An adaptive differential evolution algorithm with novel mutation and crossover strategies for global numerical optimization," *IEEE Trans. Syst., Man, Cybern., B Cybern.*, vol. 42, no. 2, pp. 482–500, Apr. 2012.

[43] A. W. Mohamed and A. K. Mohamed, "Adaptive guided differential evolution algorithm with novel mutation for numerical optimization," *Int. J. Mach. Learn. Cybern.*, vol. 10, no. 2, pp. 253–277, Feb. 2019.

[44] R. D. Zimmerman, C. E. Murillo-Sánchez, and R. J. Thomas, "MATPOWER: Steady-state operations, planning, and analysis tools for power systems research and education," *IEEE Trans. Power Syst.*, vol. 26, no. 1, pp. 12–19, Feb. 2011.

[45] C. E. Murillo-Sánchez, R. D. Zimmerman, C. L. Anderson, and R. J. Thomas, "Secure planning and operations of systems with stochastic sources, energy storage, and active demand," *IEEE Trans. Smart Grid*, vol. 4, no. 4, pp. 2220–2229, Dec. 2013.

[46] D. N. Vo and P. Schegner, "An improved particle swarm optimization for optimal power flow," in *Meta-Heuristics Optimization Algorithms in Engineering, Business, Economics, and Finance*. Hershey, PA, USA: IGI Global, 2013, pp. 1–40.

[47] Yarpiz Team. (Feb. 2019). *Nature-Inspired Algorithms*. [Online]. Available: https://www.yarpiz.com

[48] A. M. Shaheen, R. A. El-Sehiemy, and S. M. Farrag, "Solving multi-objective optimal power flow problem via forced initialised differential evolution algorithm," *IET Gener., Transmiss. Distribution*, vol. 10, no. 7, pp. 1634–1647, May 2016.

[49] T. D. de Lima, F. Lezama, J. Soares, J. F. Franco, and Z. Vale, "Modern distribution system expansion planning considering new market designs: Review and future directions," *Renew. Sustain. Energy Rev.*, vol. 202, Sep. 2024, Art. no. 114709.

GERARDO CASTAÑÓN (Senior Member, IEEE) received the B.Sc. degree in physics engineering from the Monterrey Institute of Technology and Higher Education (ITESM), Mexico, in 1987, the M.Sc. degree in physics (optics) from the Ensenada Center for Scientific Research and Higher Education, Mexico, in 1989, and the master's and Ph.D. degrees in electrical and computer engineering from The State University of New York (SUNY) at Buffalo, in 1995 and 1997, respectively. From January 1998 to November 2000, he was a Research Scientist with the Alcatel USA Corporate Research Center, Richardson, TX, USA, where he was doing research on IP over WDM, dimensioning and routing strategies for next-generation optical networks, and the design of all-optical routers. From December 2000 to August 2002, he was a Senior Researcher with Fujitsu Network Communications researching ultra high speed transmission systems. From August 2015 to July 2016, he was a Visiting Scientist with the Research Laboratory of Electronics, MIT, involved in silicon photonics integration and developing advanced telecommunication photonic devices and sensors in CMOS. He is currently a Full Professor of electrical and computer engineering with Tecnológico de Monterrey (ITESM). He has over 100 publications in journals and conferences and four international patents. He is a member of the National Research System in Mexico, a Senior Member of the IEEE Communications and Photonics Societies, and a member of the Academy of Science in Mexico. The Fulbright Scholarship supported him through the Ph.D. studies. He frequently acts as a reviewer for IEEE journals.

ANA MARIA SARMIENTO (Member, IEEE) received the B.Sc. degree in physics engineering from the Monterrey Institute of Technology and Higher Education (ITESM), Mexico, in 1989, and the master's and Ph.D. degrees in industrial engineering from The State University of New York (SUNY) at Buffalo, in 1995 and 2001, respectively. Her dissertation research was on the integrated production-logistics network optimization for the partner-chain design in agile manufacturing. Her dissertation topic received the 1998 Doctoral Dissertation Award presented by the International Society of Logistics. From 1999 to 2001, she was with i2 Technologies, Irving, TX, USA. She has been a Professor with the Department of Industrial Engineering, ITESM, Monterrey, since January 2007. Her current research interests include applying optimization methods of operations research to telecommunication networks.

ALBERTO F. MARTÍNEZ-HERRERA (Member, IEEE) is currently pursuing the Ph.D. degree in information technologies and communications with Tecnológico de Monterrey (ITESM), Monterrey, Mexico. From October 2013 to October 2014, he was an invited Ph.D. student working on cryptography with the Computer Science Department, Research Center of IPN (CINVESTAV), Zacatenco, Distrito Federal, Mexico. His research interests include applied cryptography, network security systems (secure protocols and intrusion detection systems), and network topologies. He also works on efficient hardware design techniques for cryptographic primitives and their resistance against side-channel attacks.

ALEJANDRO ARAGÓN-ZAVALA (Senior Member, IEEE) received the Graduate degree in electronics and communications engineering from Tecnológico de Monterrey, Campus Querétaro, in December 1991, and the M.Sc. degree in satellite communication engineering and the Ph.D. degree in antennas and propagation from the University of Surrey, in 1998 and 2003, respectively. He was an Engineer and a Consultant in the industry, and since 2003, he has been the Academic Director of the former IEC and ISE undergraduate programs with Tecnológico de Monterrey, Campus Querétaro, and he is in charge of ITE (all electronic engineering degrees). His research interests include mobile communications, satellite systems, high-altitude platform systems, antenna design, and indoor propagation.

FERNANDO LEZAMA (Senior Member, IEEE) received the Ph.D. degree in ICTs from the Monterrey Institute of Technology and Higher Education (ITESM), in 2014. Since August 2017, he has been a Researcher with GECAD-Polytechnic of Porto, where he contributes to applying computational intelligence (CI) in the energy domain under various problems. He has published over 100 articles in intelligent systems, energy conferences, and SCI journals. He has also been a part of the National System of Researchers of Mexico, since 2016, the Co-Chair of the IEEE CIS TF 3 on CI in the energy domain (appointed as the Chair, from 2019 to 2021). He has been involved in the organization of special sessions, workshops, and competitions at IEEE WCCI, IEEE CEC, and ACM GECCO, to promote the use of CI to solve complex problems in the energy domain.

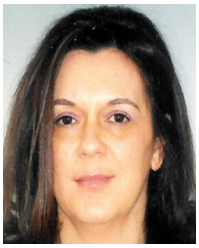

ZITA VALE (Senior Member, IEEE) received the Ph.D. degree in electrical and computer engineering and the Habilitation degree from the University of Porto, Porto, Portugal, in 1993. She is currently a Full Professor with the Polytechnic Institute of Porto, Porto. She is also the Director of the GECAD-Research Group on Intelligent Engineering and Computing for Advanced Innovation and Development. Her research interests include artificial intelligence applications, smart grids, electricity market, demand response, electric vehicles, and renewable energy sources.